MECHANISM OF OSMOTIC FLOW IN POROUS MEMBRANES

JOHN L. ANDERSON *and* DERMOT M. MALONE

From the School of Chemical Engineering, Cornell University, Ithaca, New York 14850

ABSTRACT A model for osmotic flow in porous membranes is developed from classical transport and thermodynamic relations. Mathematical expressions for the reflection coefficient as a function of solute dimension and shape, and more generally pore/bulk distribution coefficient, are derived for long cylindrical pores of circular cross section. For a rigid, spherical macromolecule the osmotic reflection coefficient equals $(1 - \Phi)^2$, where Φ is the solute distribution coefficient; this result differs significantly from expressions found in the literature. The effect of weak solute adsorption to (or repulsion from) the pore wall can also be accounted for in the derivation. The driving force for osmotic flow arises from solute-pore wall interactions which cause radial variations in concentration and concomitant gradients in pressure normal to the wall. Implications of this three-dimensionality of osmotic phenomena are discussed with particular reference to the adequacy of one-dimensional treatments in relating reflection coefficient to membrane and solute properties.

INTRODUCTION

The existence of a solute concentration gradient in an unbounded solvent does not by itself generate an appreciable volume flow. When a discriminating barrier (membrane) is placed between two solutions differing in concentration, however, a net volume flux is expected; such transport is termed "osmosis" or "osmotic flow." The classical situation occurs when the membrane is semipermeable, that is, only solvent can enter the membrane. The accepted equation for the volume flux (J_v) in such a system is

$$J_v = L_p[\Delta P_\infty - \Delta \Pi_\infty]. \tag{1}$$

The subscript ∞ denotes bulk solution conditions on each side of the membrane, and L_p is the "hydraulic coefficient," a constant for a given membrane and solvent. Strictly speaking Eq. 1 is only valid when boundary layer resistances in the bulk solution adjacent to the membrane ("unstirred layers") are negligible, that is, the bulk properties which are to be used in Eq. 1 are those which exist at the membrane-solution interface. The term $\Delta \Pi_\infty$ equals the pressure difference which would be sustained at $J_v = 0$ and is thermodynamically related to the solute concentration difference; for an ideal solution $\Delta \Pi_\infty = RT\Delta C_\infty$. Π is not a pressure by itself (1), nor is it prop-

erly described as a "solute pressure," and hence its usual name "osmotic pressure" may be misleading.

If the solute is only partially excluded from the membrane ("leaky" membrane), the osmotic contribution to flow is smaller than predicted by Eq. 1. Staverman (2) defined an osmotic reflection coefficient σ_0 for such cases:

$$J_v = L_p[\Delta P_\infty - \sigma_0 \Delta \Pi_\infty]. \tag{2}$$

Presumably σ_0 is a function of solute and membrane characteristics but relatively independent of pressure and concentration. The experimental determination of this parameter is achieved by either of two methods:

$$\sigma_0 = [-J_v/L_p \Delta \Pi_\infty]_{\Delta P_\infty = 0} = [\Delta P_\infty / \Delta \Pi_\infty]_{J_v = 0}. \tag{3}$$

A second parameter σ_f, termed the filtration reflection coefficient, was defined by Staverman with respect to convective solute flux (J_s):

$$\sigma_f = 1 - (J_s/C_\infty J_v)_{\Delta C_\infty = 0} \qquad \text{(footnote 1)}. \tag{4}$$

By formulating flux-force relationships and invoking the reciprocity theorem of Onsager, Staverman concluded that $\sigma_0 = \sigma_f$ for one-dimensional membrane transport. This reciprocal relationship has been accepted as a fundamental postulate in the development of many membrane transport models (e.g., 3–5), although experimental confirmation of its validity for the reflection coefficient is lacking.

Although accepted far earlier, it was not until recently that Eq. 1 was verified experimentally for semipermeable porous membranes (6, 7). A quite plausible model for the equivalence between pressure and osmotic driving forces was advanced independently by Mauro (8) and Ray (9). Assuming thermodynamic equilibrium (constant solvent chemical potential) at the membrane-solution boundary, the pressure must change (decrease) in going from bulk to pore solution since the solute concentration drops to zero inside the pore. Thus, a concentration difference between the bulk solutions is transformed into an intramembrane pressure difference (equal to $\Delta \Pi_\infty$) which drives the solvent flow. The situation is depicted in Fig. 1, using a long, cylindrical pore (negligible resistance to flow and mass transfer at the pore ends) as the physical model. It should be noted that Eq. 1 is valid for any membrane regardless of pore geometry and solute characteristics as long as the solute is totally excluded from the pore; however, L_p is dependent on pore geometry and solvent viscous properties.

A direct approach toward modeling osmotic flow in leaky porous membranes has been proposed by Ray (9). Essentially, the analysis for the semipermeable case ($\sigma_0 = 1$) was extended to account for solute penetration by computing the solvent chemical

[1] The experimental determination of σ_f is usually performed when $\Delta C_\infty \neq 0$. This is acceptable if it can be shown that the diffusive contribution to solute flux is negligible compared to the convective flux.

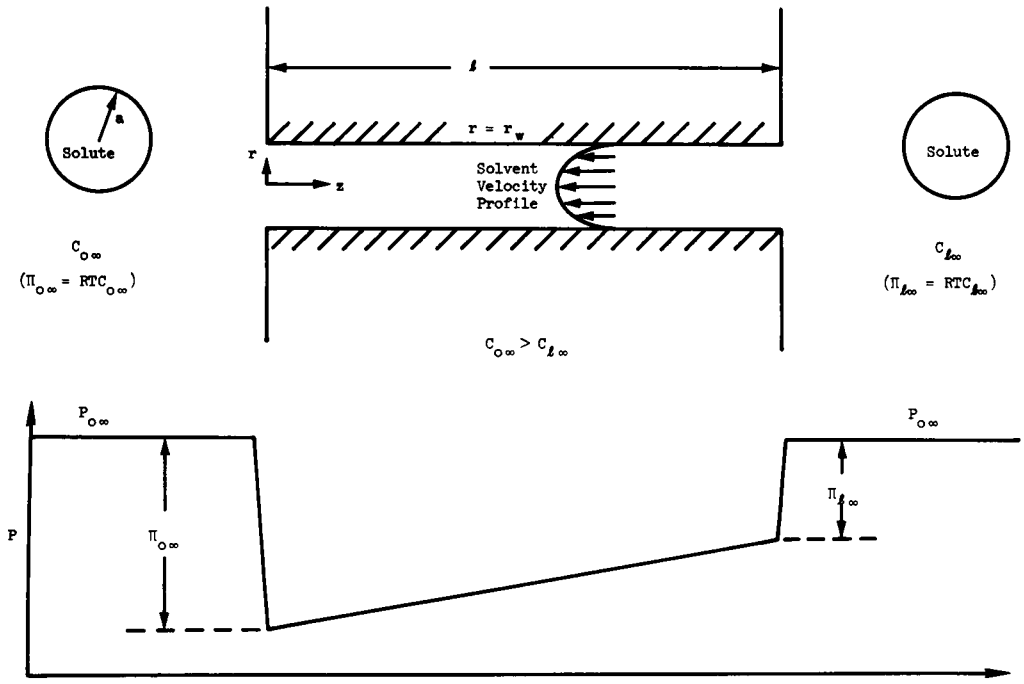

FIGURE 1 Velocity profile and pressure gradient developed within a semipermeable membrane ($\sigma_0 = 1$) of uniform cylindrical pores separating two solutions of different solute concentration at equal pressure. Solvent flux is described by Eq. 1.

potential on the basis of the *average* solute distribution coefficient (Φ) between pore and bulk solutions. The following resulted for long pores:

$$\sigma_0 = 1 - \Phi. \tag{5}$$

If only steric considerations are involved, Φ may be determined from solute and pore geometry (10). Using one-dimensional, kinetic-equilibrium analyses of transport under osmotically imbalanced conditions, Manning (11) has derived an expression for σ_0 as a function of a path-averaged pseudo-distribution coefficient, which reduces to Eq. 5 for the case of a uniform solute potential in the membrane ("square well"). He begins by assuming the existence of an arbitrary solute potential within the membrane which may only vary along the transport direction. As discussed later, such a one-dimensional treatment requires the use of area-averaged properties (that is, properties which are *assumed* uniform due to some type of averaging over an element of area normal to the transport direction), the physical interpretation of which is not always clear. In particular it will be shown that Eq. 5 is incorrect for a system of uniform cylindrical pores.

An alternate approach to relating reflection coefficient to solute and membrane characteristics has been to derive an expression for σ_f. Ferry (12) reasoned that the filtra-

tion coefficient must be determined solely by the distribution coefficient, or

$$\sigma_f = 1 - \Phi. \tag{6}$$

Renkin (13) recognized two deficiencies in the above model: first, the nonuniform, parabolic velocity profie characteristic of laminar flow is not accounted for, and second, the solute may experience an extra drag due to the proximity of the pore wall. Using a capillary pore model, he correctly modified (6) for the first deficiency but incorrectly determined the friction effect. Bean (14) and Anderson and Quinn (15) have corrected the latter by using the proper hydrodynamic formulation, the result being

$$\begin{aligned}\sigma_f &= (1 - \Phi)^2\overline{G} + (1 - \overline{G}) \\ &\doteq (1 - \Phi)^2 G_0 + (1 - G_0).\end{aligned} \tag{7}$$

$\overline{G}$ is an averaged value of the local "lag" coefficient (G) which to date has only been computed for a spherical particle located at the center line of the capillary (G_0). Bean cited experimental evidence that the approximation in expression 7 is good. If reciprocity is valid, then the above expression should also yield the correct value of osmotic reflection coefficient.

By far the most common treatment is the one-dimensional friction model. Bearman and Kirkwood (16) and Spiegler (17) proposed the use of frictional coefficients f_{ij} to linearly relate drag and relative velocity between species i and j. Others have taken this concept to apply to transport through confined liquid phases such as in a porous membrane. The pore wall effect has been introduced by *defining* coefficients f_{im}, where the m denotes membrane (pore wall). These lumped analyses are supposed to accurately describe the average frictional wall effect on solute transport. By employing the reciprocity relation, mathematical expressions for reflection coefficient have been derived in terms of these frictional coefficients (for example, 3, 4, 18–20). The validity of this one-dimensional approach to transport modeling has been critically challenged by Anderson and Quinn (15) and Mikulecky (21). Although Bean (14) attempted to relate the frictional coefficients to pore structure, the physical meaning of f_{im} is still questionable. These models shed little light on the mechanism of flow in osmotically-driven systems, especially since the assumption $\sigma_0 = \sigma_f$ is tied into the derivations. Hill (22) has presented a model consisting of "reflecting zones" arranged in series within the membrane. Equilibrium was assumed at the boundaries between zones. The parameters arising in this analysis (e.g., zone thickness) are empirical in nature and say little about the relationship of σ_0 to membrane structure. A particular criticism of Hill's treatment is that the mechanism of flow in a zone into which solute can penetrate to a limited extent was not dealt with satisfactorily. In fact, it appears that he assumed the flow must be purely diffusive through a zone (pore) into which the solute may penetrate; arguments to the contrary are presented here.

In this paper the mechanism of osmotic flow in porous membranes is examined directly by computing the average volume flux in terms of the pressure and concentra-

tion driving forces. No use of the reciprocal relation ($\sigma_0 = \sigma_f$) is made. The conceptual basis of this work is that the thermodynamic effect of the pore wall on the solute determines the coupling between solute concentration difference and bulk flow. Utilizing a system of long, parallel, cylindrical pores as the model membrane, a quantitative relationship between reflection coefficient and solute characteristics (dimension, shape, affinity for the pore wall) is developed. Only intrinsic membrane transport characteristics are of interest, so that pore end effects (i.e. resistance to transport) are neglected. The solvent is assumed a continuum with respect to pore dimensions; thus, the fluid transport is viscous rather than diffusive in nature (14, 23, 24). A general model is first derived using an arbitrary solute potential which varies radially within the pore and only affects the solute distribution. The concept involved is quite similar to that used by Derjaguin et al. (25) for flow induced by solute adsorption to the walls of macroscopic capillaries. Subsequent sections deal with two forms of this solute potential: steric exclusion and dispersion interactions (adsorption). The steric effect is examined for both spherical and nonspherical macrosolutes. Finally, a discussion of general (noncapillary) heterogeneous membranes and the validity of one-dimensional models is presented. This paper emphasizes that three-dimensional variations of solute concentration within a pore have a dominant influence on transport rates in osmotically-driven systems and the magnitude of the osmotic reflection coefficient is highly dependent on solute dimension and shape as well as membrane structure.

OSMOTIC FLOW IN A MEMBRANE OF CIRCULAR CYLINDRICAL PORES

If the solute molecule is small enough to enter the pore, concentration and pressure variations must be examined more carefully than one might suppose. The significance of a pore is its confinement of the fluid phase, and hence the pore wall is expected to be the origin of the so-called "restricted transport" effect occurring within the fluid phase. Although seemingly obvious, this fact is usually overlooked in the development of transport expressions for porous media. A physically meaningful model for describing transport in small pores ("small" in the sense that the pore radius is of the same order of magnitude as the dimension of at least one of the transported species) must then begin with a proper account of how conditions vary *normal* to the pore wall. As is shown below, static but nonuniform conditions (concentration, pressure) along the radial direction of a permeable cylindrical pore provide the driving force for osmotic flow.

The model begins with a long, cylindrical pore of radius r_w and length l as shown in Fig. 1. The total transport resistance is assumed to be within the pore itself ($l/r_w \rightarrow \infty$), so that a state of thermodynamic equilibrium between the pore and bulk fluid phases may be properly assumed at both ends. Furthermore, equilibrium conditions are assumed to exist in the radial direction for any z (see Appendix). A solute potential energy field $\phi(r)$ which controls the radial distribution of solute may exist within the pore. Such a field would presumably originate at the pore wall, some examples being

London dispersion interactions, infinite repulsion barriers due to steric limitations, and electrical double layer interactions. The potential is assumed to be only a function of radial position (r) (footnote 2) and is defined relative to the bulk phase where its value is zero. Solute-solvent interactions in the pore are assumed identical to those in the bulk solution, and thus $\phi(r)$ represents totally a wall effect on the solute; the solvent is unaffected by the potential field.

Because radial mechanical equilibrium exists within the pore, the Gibbs-Duhem equation can be used to relate pressure and potential gradients:

$$(\partial P/\partial r) + C(\partial \phi/\partial r) = 0, \tag{8}$$

where C is the solute concentration which may be a function of both r and z. The solute chemical potential is also constant radially as a consequence of thermodynamic equilibrium. Assuming a constant activity coefficient of solute as well as low volume fraction, the Boltzmann equation is valid:

$$C(r,z) = C_0(z) \exp\left[-\frac{(\phi(r) - \phi(0))}{RT}\right]. \tag{9}$$

The subscript zero designates the pore center line ($r = 0$). Substitution of Eq. 9 into 8 and subsequent integration yields

$$P(r,z) = P_0(z) - \Pi_0(z)[1 - e^{-(V(r)-V(0))}], \tag{10}$$

where $\Pi_0(z)$ is the "osmotic pressure," $RTC_0(z)$, and $V(r)$ is the dimensionless potential, $\phi(r)/RT$. The above expression illustrates the coupling between solute concentration and pressure which generates the driving force for bulk flow.

Reynolds numbers are extremely small so the quasi-static, inertial free form of the Navier-Stokes equation correctly describes momentum transfer. The long pore assumption justifies use of the following simplified equation for the axial velocity $U(r,z)$ (see Appendix):

$$(\eta/r)(\partial/\partial r)[r(\partial U/\partial r)] - (\partial P/\partial z) = 0. \tag{11}$$

Implicit in the use of the above equation are the following: (a) the solvent is a continuum compared with the scale of the pore radius; (b) the solute volume fraction is small, implying that the viscosity η is constant and approximately equal to that of the pure solvent (see Wang and Skalak [26] for the usual magnitude of the correc-

[2] The potential may also depend on orientation if the solute is nonspherical and on extent of deformation if not rigid.

tions to viscosity); (*c*) the small force (pressure) resulting from a slightly unbalanced diffusive mass flow due to unequal solute and solvent specific volumes is neglected (27). Substituting for P from Eq. 10 gives

$$(\eta/r)(\partial/\partial r)[r(\partial U/\partial r)] - P_0'(z) + \Pi_0'(z)[1 - e^{-(V(r)-V(0))}] = 0, \qquad (12)$$

where the prime denotes a derivative with respect to z. By integrating the above twice in r and utilizing the classical no slip ($U(r_w, z) = 0$) boundary condition, the following is obtained for the axial velocity profile:

$$U = -\frac{(r_w^2 - r^2)}{4\eta} P_0'(z) + \frac{\Pi_0'(z)}{\eta} \int_r^{r_w} \frac{dy}{y} \int_0^y x[1 - e^{-(V(x)-V(0))}]\,dx. \qquad (13)$$

Besides the fact that the velocity is dependent on the *axial* concentration gradient ($\Pi_0'(z)$) via the *radial* variation in potential (the double integral), note should be made of the shape of the velocity profile. Specifically, the second term on the right-hand side is in general nonparabolic, and hence the velocity profile for osmotic flow may differ considerably from a pressure-driven flow even if the average velocities are the same for both. The same conclusion is reached for electroosmotic flow (the potential field is somewhat more complicated in this case) by Wyman and Kostin (28). This result has a significant consequence as demonstrated later. In general $P_0'(z)$ and $\Pi_0'(z)$ are not constant, so that simultaneous solution of the mass flux equation for solute is required to compute the actual velocity profile.

It should be emphasized that $J_v = 0$ (or $\bar{U} = 0$) in Eq. 3 does not imply mechanical equilibrium ($U(r, z) = 0$) along the axial direction within the pore except for semipermeable membranes ($\sigma_0 = 1$). The imbalance in point velocity at zero *net* flow is due to the difference in velocity profile (shape) between pressure-driven and osmotic-driven flow as mentioned above. In fact if it were assumed that $U(r, z) = 0$ everywhere in the pore at $\bar{U} = 0$, then Eq. 12 would lead to the following impossible relation:

$$P_0'(z)/\Pi_0'(z) = 1 - e^{-(V(r)-V(0))}.$$

The left-hand side of the above is presumably only a function of z while the right-hand side is only a function of r. Thus, the expression $(\eta/r)\,(\partial/\partial r)\,(r[\partial U/\partial r])$ must be a function of both r and z even at $\bar{U} = 0$. No violation of fluid continuity is made by postulating that the axial point velocity due to osmosis varies with z since the actual continuity expression is

$$\vec{\nabla} \cdot \vec{U} = 0 = (\partial U/\partial z) + (\partial W/\partial r),$$

where W is the radial fluid velocity which is properly neglected in the radial momentum balance (Eq. 8) due to the large value of pore length/radius. What we are saying here is that a very small radial velocity component (W) exists in osmotic flow systems to

compensate for a nonzero $\partial U/\partial z$, but its magnitude (more appropriately, $\partial^2 W/\partial z^2$) is trivial compared with the radial pressure and potential gradient in Eq. 8.

The average fluid velocity ($\overline{U}$) is found by integrally averaging Eq. 13 over the total pore area:

$$\overline{U} = -(r_w^2/8\eta)P_0'(z) + (\Pi_0'(z)B/\eta r_w^2), \tag{14A}$$

$$B = \int_0^{r_w} 2r\mathrm{d}r \int_r^{r_w} \frac{\mathrm{d}y}{y} \int_0^y x[1 - e^{-(V(x)-V(0))}]\,\mathrm{d}x. \tag{14B}$$

Since by continuity $\overline{U}$ is a constant independent of z, Eq. 14 A) may be directly integrated along the pore axis to obtain

$$\overline{U} = (L_p/\alpha)\{[P_0(0) - P_0(l)] - [\Pi_0(0) - \Pi_0(l)](8B/r_w^4)\}. \tag{15}$$

L_p is the hydraulic coefficient, equal to $\alpha r_w^2/(8\eta l)$ for a cylindrical pore, and α is the pore volume fraction of the membrane. The above expression is not useful as it stands since it makes use of intramembrane rather than bulk pressure and osmotic differences. The Boltzmann and Gibbs-Duhem relations are used at the pore ends to introduce bulk parameters into the model:

$$\Pi_0(0) = \Pi_{0\infty}\, e^{-V(0)}, \tag{16A}$$

$$\Pi_0(l) = \Pi_{l\infty}\, e^{-V(0)}, \tag{16B}$$

$$P_0(0) = P_{0\infty} - \Pi_{0\infty}[1 - e^{-V(0)}], \tag{16C}$$

$$P_0(l) = P_{l\infty} - \Pi_{l\infty}[1 - e^{-V(0)}]. \tag{16D}$$

The subscript ∞ denotes bulk fluid phase. Substitution of these relations into Eq. 15 gives the desired result:

$$J_v = L_p[\Delta P_\infty - \sigma_0 \Delta\Pi_\infty], \tag{17A}$$

$$\sigma_0 = 1 - \frac{8}{r_w^4} \int_0^{r_w} 2r\mathrm{d}r \int_r^{r_w} \frac{dy}{y} \int_0^y x\exp(-V(x))\,\mathrm{d}x. \tag{17B}$$

where Δ means side 0 minus side l, and J_v is positive when the flow is from side $0 \rightarrow l$. Note that the membrane volume flux (J_v) has been substituted for the pore volume flux ($\overline{U}$) times the pore area (volume) fraction (α). The reflection coefficient depends on both the pore radius as well as the solute potential profile. Subsequent sections deal with two contributions to the potential: steric exclusion and dispersion interactions (solute adsorption). A semipermeable membrane is modeled by letting $V(r) \rightarrow \infty$ so $\sigma_0 \rightarrow 1$, while for a large pore which does not discriminate between solute and solvent $V(r) \rightarrow 0$ and hence $\sigma_0 \rightarrow 0$.

The several assumptions necessary for the validity of Eq. 17 B are now summarized. More detailed arguments supporting the existence of equilibrium radially within the

pore are given in the Appendix, but qualitatively the requirement is stated as $l \gg r_w$. This long pore assumption also justifies neglect of end resistance effects at the pore-bulk solution interface, so that pressure and concentration changes in going from the bulk solution just outside the pore to the solution just inside can be related via the Gibbs-Duhem and Boltzmann expressions (Eq. 16 *A-D*) without need of rate expressions for mass and momentum transport. The potential energy $\phi(r)$ is assumed to only apply to the solute, implying that solvent-pore wall interactions are absent. This implication would be satisfied if the solvent dimension were much smaller than r_w; the continuum hypothesis necessary to use the Navier-Stokes equation and associated boundary conditions would also be satisfied if this were the case. A constant viscosity (approximately that of the pure solvent) is assumed in the derivation, so that solute volume fraction *in the pore* must be "small" (say less than 10% [26]), and strong adsorption resulting in solute immobility at the pore wall must not occur (in which case η would become very large at the wall). Finally, use of the Boltzmann equation requires the solute activity coefficient to be constant. In summary, Eq. 17 *B* is specific for a long, circular cylindrical pore and a solute molecule which is much larger than the solvent, is present at small volume fraction in the pore fluid, and interacts with the pore wall without losing its axial mobility.

STERIC EXCLUSION WITH SPHERICAL SOLUTE MOLECULES

The simplest yet still physically meaningful application of Eq. 17 *B* is to a spherical macromolecule that only interacts sterically with the pore wall. That is to say, the solute potential is zero for all values of r available to the center of mass of the solute, while it is infinite very close to wall where the solute is prohibited due to its size alone. The concept of steric exclusion for rigid macromolecules is nicely described by Giddings et al. (10). In their treatment the pore walls are defined as infinite potential barriers located one projected solute dimension away from the physical boundary. The potential is a step function going from zero when the solute center is located further away from the wall than the barrier ("accessible" region) to positive infinity when closer to the wall ("excluded" region). A configuration integral over the pore volume and all solute orientations results, which in a simplified interpretation means that the apparent distribution of solute between pore and bulk fluid is given by the ratio of accessible-to-total pore volume. If the solute molecule is spherical, orientation considerations vanish from the computation and the partitioning is well defined by an excluded region adjacent to the pore wall whose thickness equals the solute radius.

Assume that the solute molecule is a rigid sphere of radius a. The general pore model of the previous section is used. The solute dimensionless potential is given by the steric effect alone:

$$V(r) = 0 \qquad 0 < r \leq r_w - a$$

$$V(r) \rightarrow \infty \qquad r > r_w - a \quad .$$

The reflection coefficient is evaluated by utilizing a step function (S) determined by

this potential profile:

$$e^{-V(x)} = 1 - S[x - (r_w - a)], \tag{18}$$

and the triple integration in Eq. 17 *B* yields

$$\sigma_0 = [1 - (1 - \lambda)^2]^2, \tag{19}$$

where λ equals a/r_w, the ratio of solute-to-pore radius. The apparent (measurable) pore-bulk distribution coefficient Φ is $(1 - \lambda)^2$, so Eq. 19 may be rewritten as

$$\sigma_0 = (1 - \Phi)^2. \tag{20}$$

Although the above appears quite general, its applicability is still restricted to spherical macromolecules in long, cylindrical pores with inert walls as discussed later.

A descriptive picture of the steric effect is given in Fig. 2. The pore fluid can be thought of as a composite of two phases: an inner core of radius $r_w - a$ for which the solute equilibrium distribution with respect to the bulk fluid is unity, and an excluded annulus of thickness a adjacent to the pore wall containing no solute. This radial partitioning establishes an equilibrium pressure drop across the imaginary boundary $r = r_w - a$:

$$P_e(z) = P_c(z) - \Pi(z), \tag{21}$$

where the subscripts e and c represent excluded and core regions, respectively. In this

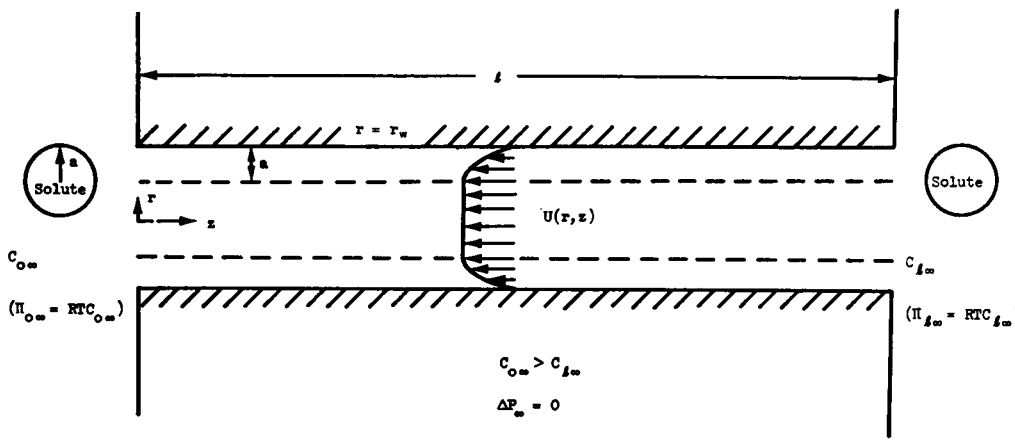

FIGURE 2 Approximate velocity profile $U(r,z)$ developed within a permeable membrane of uniform circular cylindrical pores separating solutions of spherical solute molecules at different concentrations. Only steric pore wall-solute interactions are assumed to exist (no adsorption). The dashed lines separate the core (accessible) from the excluded region. Since the bulk solutions are at equal pressure, the core velocity is expected to be very flat and approximately equal to $U_0(z)$ which is given in Eq. 22 *B*.

expression $\Pi(z)$ is the actual thermodynamic osmotic pressure one would measure at core concentration $C(z)$. The mechanism for osmotic flow is then easily understood from Eq. 21. The steric exclusion of solute near the pore wall creates an abrupt pressure change proportional to the solute concentration; thus, an axial concentration gradient in the core establishes an axial pressure gradient in the excluded region which "pushes" the fluid through the pore. The equation for the velocity profile is derived from Eq. 13; for the core region the integration gives

$$U_c = -[(r_w^2 - r^2)/4\eta]P_c'(z) + U_0(z) \qquad (22A)$$

$$U_0(z) = (r_w^2/4\eta)[1 - (1 - \lambda)^2 + 2(1 - \lambda)^2 \ln(1 - \lambda)]\Pi_0'(z). \qquad (22B)$$

As mentioned before, exact determination of $P_c'(z)$ and $\Pi'(z)$ requires the solution of the mass flux equation for solute, which is coupled to the velocity profile. If there is no pressure difference between bulk solutions on either side of the membrane, $P_c'(z)$ is expected to be small (but not zero) and the core velocity profile is relatively flat ($U_c \sim U_0(z)$). The osmotic flow thus resembles a "plug" flow such as found in electroosmosis and is quite different from the parabolic shape resulting when the flow is pressure-driven. As a result, a zero net flow ($J_v = 0$) sustained by a balance between opposing mechanical and osmotic pressure differences is not a true equilibrium situation since the local pore velocity ($U(r,z)$) is generally nonzero. It should be noted that a one dimensional analysis predicts intramembrane equilibrium at zero net flow because identical flow mechanisms for pressure and osmotic driven systems are implicitly assumed (11).

In the above model the pressure drop near the wall is given a step function representation which may be challenged on physical grounds. The distance required to establish the equilibrium condition described by the Gibbs-Duhem equation is probably one or two solvent diameters, the solvent exchange being primarily diffusive across the boundary $r = r_w - a$. Solvent attempts to move from the excluded to the core region, creating a pressure deficiency in the former large enough to balance thermodynamically the concentration difference. If the solvent molecular dimension is much smaller than the solute's, this steep but continuous change in pressure is adequately described by a step function. A correction for the finite radial pressure gradient at the transition between the core and excluded regions can be introduced mathematically for small solutes, but the resulting calculations for σ_0 would be questionable anyway since the solvent continuum hypothesis would be violated.

As an aside, Eq. 21 predicts that the pressure in the excluded region can attain negative absolute values if the osmotic term is large. Such an occurrence is feasible since liquids are known to be able to support tension (negative pressure) up to many atmospheres in the absence of vapor nucleation sites (11, 29, 30). For example, such a situation can be achieved readily in thin liquid films due to the capillarity effect with curved gas-liquid interfaces (i.e. the LaPlace equation), and Mauro (31) has measured negative absolute pressures in a special osmometer.

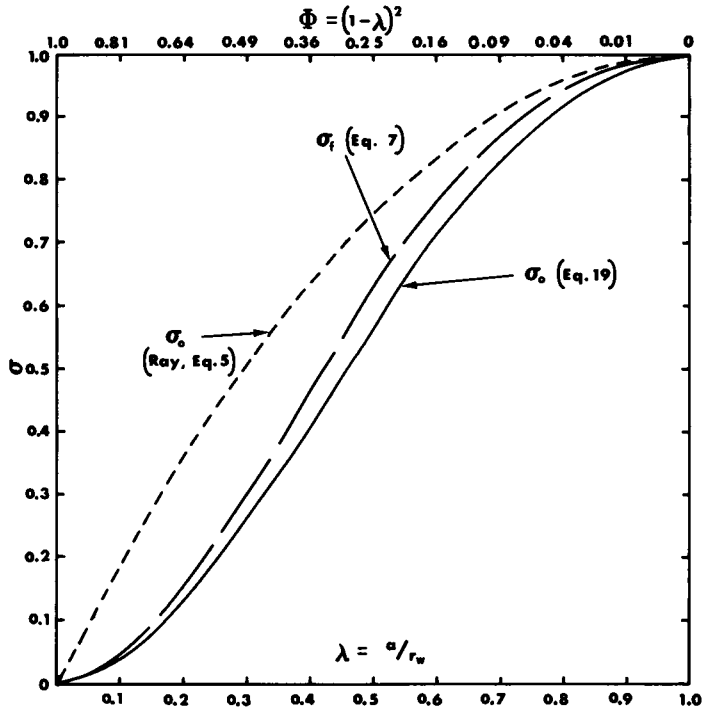

FIGURE 3 Reflection coefficient for membranes containing uniform cylindrical pores (radius r_w) versus solute-to-pore radius (λ) and solute pore/bulk distribution coefficient (Φ). The solute is assumed to be a spherical macromolecule (radius a) which only interacts sterically with the pore wall (no adsorption).

The osmotic reflection coefficient as computed from Eq. 19 is plotted against solute-to-pore radius (λ) in Fig. 3. Included for comparison is the result obtained by Ray (Eq. 5) which is seen to differ considerably from our expression. The difficulty in accepting Ray's result is that he treats the solute distribution within the pore at any axial position (z) as uniform when actually the radial variation is quite pronounced. The application of point equilibrium principles (Gibbs-Duhem, equalization of chemical potentials) in a lumped-parameter, one-dimensional model when the system is in fact distributed has no thermodynamic validity, and the result of such an analysis can only be regarded as approximate at best. To underline the error in Ray's model, consider a membrane with a tapered pore of radius r'_w and r''_w at the ends. Suppose that the bulk solutions on each side are identical in pressure and concentration. By the one-dimensional reasoning that Ray followed, an axial pressure drop inside the pore is predicted since the solute pore-bulk partition coefficient differs between the ends due to dissimilar steric factors ($r'_w \neq r''_w$). A bulk flow should then result in the direction of the smaller pore radius, a blatant violation of the second law of thermodynamics. If our model were applied to this geometry, however, no such internal pressure gradient or flow would be predicted for the symmetric system; the only pressure variation arising would

be normal to the pore wall and thus would not induce a flow. Manning's development does not suffer from this symmetry failure due to proper analysis of changes along the direction of transport.

The filtration coefficient (σ_f) as calculated from Eq. 7 is also plotted in Fig. 3. Although the differences are not great, σ_0 and σ_f are not identical as assumed in numerous linear transport models (2, 5, 18). The basis for this equivalence is the reciprocal relation of Onsager (32) which postulates that the matrix of phenomenological coefficients which linearly relates fluxes to driving forces is symmetric. Several theorists (33–35) raise objections to the universal applicability of this postulate to macroscopic systems and adopt the position that the reciprocity assumption should be subject to experimental confirmation for a particular transport situation. We are unaware of any such published confirmation for a partially reflecting porous membrane; therefore, the fact that σ_f and σ_0 (as calculated from Eqs. 7 and 19) are not identically equal does not necessarily imply that one is in error. However, it is emphasized here that certain approximations made in deriving the expressions 7 and 19 may account for the nonequivalence of the two reflection coefficients and hence these results cannot be used as evidence supporting the invalidity of Onsager's relation for this system. Specifically, the pore-averaged lag coefficient ($\overline{G}$) is approximated by the centerline value (G_0). This lag coefficient is less than unity and represents the effect of the pore wall on the viscous interaction between solute and solvent. In the derivation of σ_0 such interactions are neglected (i.e. the pure solvent viscosity is used to characterize the pore momentum transport), the result being a slight underestimation of the reflection coefficient since the presence of solute would probably raise the local apparent viscosity above the pure solvent value. Neglect of this possible solute effect on viscosity seems justified since in osmotic flow (Fig. 2) the velocity profile is relatively flat over the region accessible to the solute (implying negligible solute-solvent viscous interaction), whereas the steepest gradient occurs at the pore well where solute is excluded.

STERIC EXCLUSION—ECCENTRIC SOLUTE SHAPES

To properly include the effect of shape on the reflection coefficient of a rigid macromolecule, it is necessary to introduce solute orientation into the potential energy, again assuming a cylindrical pore:

$$V(r) = 0 \qquad 0 \leq r \leq r_w - \beta(a,\Psi)$$
$$V(r) \to \infty \qquad r > r_w - \beta(a,\Psi) \quad ,$$

where Ψ is the Eulerian angular orientation of the solute molecule with respect to a fixed coordinate system with origin at the solute center of mass (see ref. 36, p. 205), and $2a$ is the "mean external length" of the solute (10). The parameter β equals the closest possible approach of the solute center of mass to the pore wall and is a function of size and orientation. When the center of mass is located at β from the pore wall, the solute just makes contact with the wall, and since it is rigid and the wall impermeable it

can get no closer. For a sphere β equals the radius (a) for all orientations. The above potential profile again leads to a step function for the exponential term in Eq. 17 B, but now it must be integrated over all solute orientations because of the randomizing effect of Brownian motion:

$$\sigma_0 = 1 - \frac{8}{r_w^4} \int_0^{r_w} 2r\mathrm{d}r \int_r^{r_w} \frac{\mathrm{d}y}{y} \int_0^y x\mathrm{d}x \int_\Psi \{1 - S[x - (r_w - \beta)]\}\,\mathrm{d}\Psi, \quad (23)$$

where the orientation variables are normalized:

$$\int_\Psi \mathrm{d}\Psi = 1.$$

The order of integration between Ψ and r is unimportant, so the above may also be written as

$$\sigma_0 = 1 - \frac{8}{r_w^4} \int_\Psi \mathrm{d}\Psi \int_0^{r_w} 2r\mathrm{d}r \int_r^{r_w} \frac{\mathrm{d}y}{y} \int_0^y x\{1 - S[x - (r_w - \beta)]\}\mathrm{d}x. \quad (24)$$

Remembering that β is a function of Ψ, the reflection coefficient is then computed from the above:

$$\sigma_0 = \int_\Psi [1 - (1 - \beta/r_w)^2]^2\,\mathrm{d}\Psi. \quad (25)$$

The apparent pore-bulk distribution coefficient is given by (10)

$$\Phi = \int_\Psi (1 - \beta/r_w)^2\,\mathrm{d}\Psi. \quad (26)$$

Define the "deviation" δ as

$$\delta \equiv \Phi - (1 - \beta/r_w)^2. \quad (27)$$

Eqs. 25–27 are then combined to obtain

$$\sigma_0 = (1 - \Phi)^2 + \int_\Psi \delta^2\,\mathrm{d}\Psi. \quad (28)$$

A comparison of Eq. 20 and 28 shows that from steric considerations alone a non-spherical solute exhibits a higher osmotic reflection coefficient than a spherical solute even if the distribution coefficient is the same for both.

The reflection coefficient can be computed for a solute of any shape directly from Eq. 25 if β is written as a function of the orientation coordinates. A rather simple but useful estimate of the square deviation integral in Eq. 28 may be made if the solute shape can be approximated by a capsule which is composed of a cylindrical body with a hemispherical cap at each end. Let $2a_1$ equal the total capsule length and $2a_2$ the

diameter of the cylindrical body and hemispherical caps; the eccentricity ϵ is defined as a_2/a_1, so that for a sphere $\epsilon = 1$ and for a needle $\epsilon = 0$. As demonstrated by Giddings et al. (10), this model shape is much simpler mathematically than a prolate spheroid but probably as meaningful physically. They obtain for the mean external length the simple relation

$$2a = a_1 + a_2. \tag{29}$$

From Fig. 7 of their paper a good approximation for the distribution coefficient of such shaped solute molecules can be derived:

$$\Phi \doteq (1 - \lambda)^2, \tag{30}$$

where again λ is a/r_w. An average deviation can be written from Eq. 29 and 30 by algebraically averaging the extremes, $\beta = a_1$ and $\beta = a_2$:

$$\delta_{ave} = \frac{1}{2}\left\{\frac{|(1 - a_1/r_w)^2 - (1 - a/r_w)^2|}{2} + \frac{|(1 - a_2/r_w)^2 - (1 - a/r_w)^2|}{2}\right\}$$

$$= \lambda \frac{(1 - \epsilon)}{(1 + \epsilon)}\left[1 + \frac{\lambda(1 - \epsilon)}{2(1 + \epsilon)}\right]. \tag{31}$$

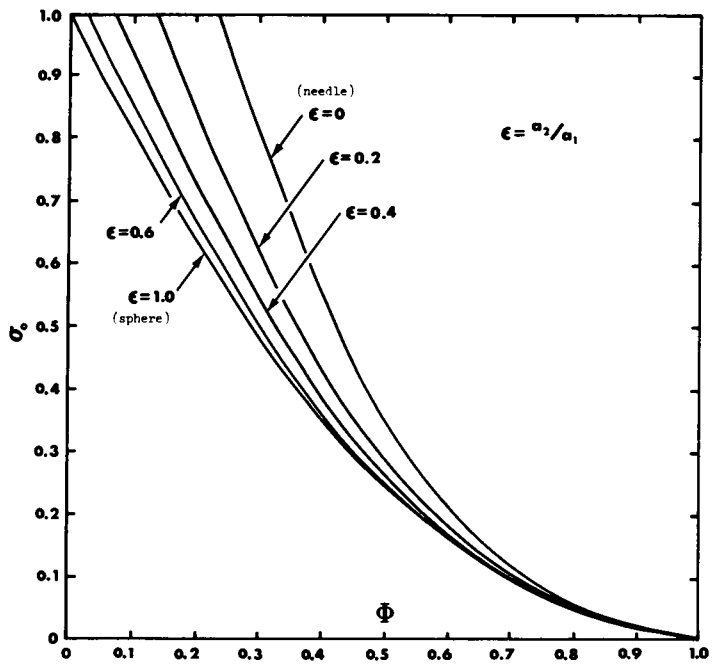

FIGURE 4 Reflection coefficient for capsule-shaped particles of different eccentricities (ϵ) as a function of solute distribution coefficient (Φ) as computed from Eq. 32. Only steric interactions are considered.

Substitution of this into Eq. 28 gives an estimate of σ_0:

$$\sigma_0 \approx (1 - \Phi)^2 + \delta_{ave}^2. \tag{32}$$

Eq. 32 is plotted in Fig. 4 to illustrate the larger reflection coefficients expected for eccentric solutes from steric factors alone. Of course σ_0 can never exceed unity, and thus except for the spherical case ($\epsilon = 1$) the accuracy of these curves as $\Phi \rightarrow 0$ is suspect. The higher osmotic activity of nonspherical solutes is due to the greater exponential weighting of β than occurs in the expression for the distribution coefficient; that is, the reflection coefficient is an orientation-averaged value of the square of the excluded volume, whereas the distribution coefficient is computed from the average of the first power. Eqs. 25 and 28 have been derived assuming that all allowable orientations of the solute molecule are equally probable, a good assumption in view of the small velocity gradients characteristic of osmotic flows.

EFFECTS OF SOLUTE ADSORPTION

The solute may experience an attraction to or repulsion from the pore wall caused by London dispersion and electrical double layer forces (37). The steric effect would still be present, however. Such interactions will now be included in the calculation of σ_0 for a rigid, spherical macromolecule of radius a in the cylindrical pore. Only solute adsorption is considered; the principle is identical for repulsion.

The dimensionless solute potential is divided into a steric component, identical to that presented earlier, and an adsorption component $V^*(r)$:

$$V(r) = V^*(r) \qquad 0 \le r \le r_w - a$$
$$V(r) \rightarrow \infty \qquad r > r_w - a \quad .$$

The following form is used for the adsorption potential:

$$V^*(r) = \frac{A}{(r_w - r)^n}, \tag{33}$$

where A is negative and related to a Hamaker constant, and n is usually in the range 0–6. Eq. 17 B is written as:

$$\sigma_0 = 1 - \frac{8}{r_w^4} \int_0^{r_w} 2r\,dr \int_r^{r_w} \frac{dy}{y} \int_0^y x[1 - S(x - (r_w - a))] \cdot e^{-V^*(x)}\,dx. \tag{34}$$

Values of σ_0 have been numerically calculated from the above using the adsorption potential in Eq. 33 with various values of A and n. The results are plotted in Figs. 5 and 6. The parameter V_w^* is the potential energy when the solute touches the pore wall:

$$V_w^* = V^*(r_w - a) = A/a^n.$$

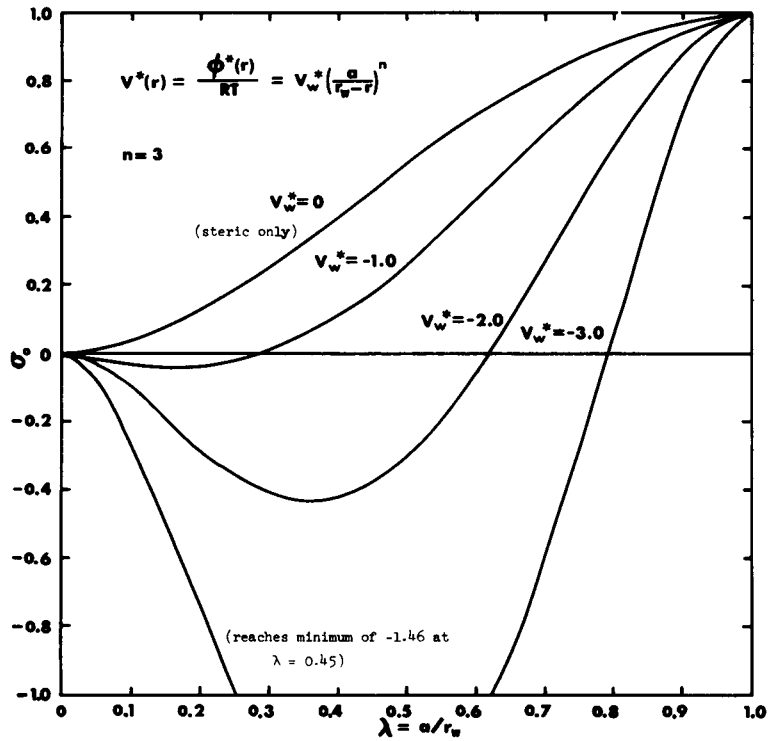

FIGURE 5 Osmotic reflection coefficient (σ_0) versus solute-to-pore radius (λ) for different wall adsorption potentials (V_w^*). Steric interactions between the (spherical) solute and pore wall are included in the calculations.

These figures show that adsorption may have a rather large effect on the solute reflection, although steric influences are dominant as $\lambda \to 1$. A negative σ_0 implies that the net flow is in the direction from concentrated to dilute side of the membrane, and such cases have been observed experimentally (3, 11, 38). Derjaguin et al. (25) have observed bulk flow from concentrated to dilute solutions when the solute adsorbed to the walls of micron-sized capillaries. No principle of thermodynamics is violated by such behavior. The case $n = 0$ corresponds to the one-dimensional treatment of Ray (9) and Manning (11) with steric exclusion included; as $\lambda \to 0$, the steric effect disappears and $\sigma_0 \to (1 - e^{-V_w^*})$, in agreement with Eq. 5 since $\Phi = e^{-V_w^*}$ at this limit. The parameter limits $n \to \infty$ and $V_w^* \to 0$ converge to the steric curve (Eq. 19).

A relatively weak solute-pore wall interaction can produce a quite significant deviation from the value for σ_0 computed from steric considerations alone: when $V_w^* = -1$ the equilibrium solute concentration at the wall is less than three times the bulk concentration. Stronger adsorption may not follow a monotonic trend of decreasing σ_0 as implied by Fig. 5, however, since the effect of solute concentration on fluid viscosity has been neglected. For example, irreversible adsorption ($V_w^* \ll -1$) would not result in a large negative reflection coefficient as predicted from the calculations presented

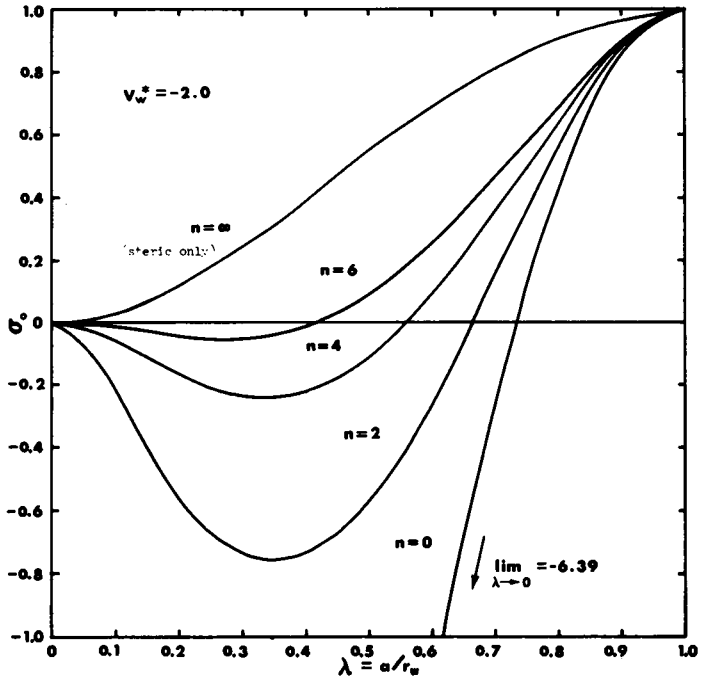

FIGURE 6 Osmotic reflection coefficient versus solute-to-pore radius for different adsorption potential exponents (n).

here because of the immobility of the solute which is "stuck" to the pore wall. Rather, the irreversibly adsorbed solute would decrease the effective pore radius and thus tend to increase σ_0 even above the steric curve. Where to draw the line between mobile and immobile adsorbed solute is not certain; in fact, it is likely that no sharp differentiation exists. An approximate criterion could perhaps be established from a hydrodynamic analysis of the concentration dependence of solution viscosity near solid boundaries, but as yet this has not been done and no attempt is made here. The calculations plotted in Figs. 5 and 6 are only supposed to show that a *weak* attraction between solute and pore wall should decrease the reflection coefficient from the value based solely on steric factors and may even result in a negative value implying flow from concentrated to dilute solutions. The significance of these results is that σ_0 may not be uniquely determined by pore and solute dimension as is often assumed (39).

MEMBRANES WITH ARBITRARY PORE STRUCTURE

It is recognized of course that the circular cylindrical capillary is not a realistic pore model in the structural sense. The rather common usage of this model derives from both its relative simplicity as well as the inherent difficulties confronting mass and momentum transport analysis in noncylindrical, intersecting channels. Although in some cases this idealized model yields quantitative results which seem to adequately

describe transport in real porous membranes, its real contribution is the elucidation of the fundamental processes (mechanisms) important to the phenomenon of interest. Furthermore, it is expected that a transport model which is general in nature is certainly valid for the simplified system of a series of uniform, parallel, cylindrical pores, so that exact results derived from such a model can also serve as a check on the validity of models claiming general applicability. The cylindrical pore represents a continuous fluid volume which is bounded by a rigid surface (pore wall) at which thermodynamic changes occur, either by passive steric repulsion or dispersion forces. These solute-surface thermodynamic interactions should be the same for the real and model systems, but the resulting total volume and species fluxes depend on the three-dimensional pore structure.

A rigid, heterogeneous ("porous") membrane consists of two distinct, continuous phases, generally an impermeable solid network and liquid solution (fluid). The solid network must be continuous throughout the membrane to maintain stability. (If in fact the solid phase is discontinuous, that is, one must cross the fluid phase in traversing from one side of the membrane to the other, then the membrane is actually a "suspension" and must be contained by a support.) Thus, a well-defined, continuous interior surface ("pore wall") exists within the membrane, and it is possible to traverse the entire membrane thickness by any of an infinite number of paths which always remain at the fluid-pore wall interface. According to the theory proposed here (assuming only steric repulsion of solute at the interior surfaces), the solute is excluded from regions near the pore wall, the region thickness being equal to one-half the solute dimension, and the pressure at the wall is consequently reduced by a proportionate amount to equilibrate the solvent activity. On the average, then, a solute concentration gradient in the z direction (normal to the plane of the membrane) creates *on the average* an opposite pressure gradient in the z direction adjacent to the fluid-pore wall interfaces (the excluded regions) which pushes the fluid through the membrane. As shown below, however, determination of the osmotic flow (i.e., σ_0) requires integration of the fluid velocity profile as determined from the Navier-Stokes equation.

Consider a cylindrical pore of arbitrary but *constant* cross section whose boundary (pore wall) is defined by $f(x,y) = 0$, where (x,y) are rectilinear coordinates in the plane of the cross section. Again the pore is assumed very long so that the assumption of mechanical equilibrium in the (x,y) plane is valid:

$$(\partial P/\partial x) + C(\partial \phi/\partial x) = 0, \tag{35A}$$

$$(\partial P/\partial y) + C(\partial \phi/\partial y) = 0. \tag{35B}$$

If the origin (0,0) is a point of finite solute potential ϕ_0, then the above equations may be integrated using the Boltzmann expression as was done in deriving Eq. 10:

$$P = P_0(z) - \Pi_0(z)[1 - e^{-(V(x,y)-V_0)}], \tag{36}$$

where again V is the dimensionless solute potential. Now if the Navier-Stokes equation

is integrated over a fluid volume element bounded by the surfaces $z = z_1$, $z = z_2$, and $f(x,y) = 0$,

$$\int \left(\eta \nabla^2 U - \frac{\partial P}{\partial z} \right) dV = 0 \tag{37}$$

(∇^2 is the LaPlacian operator and U is the fluid velocity in the z direction), the following is readily obtained (40) by using the Gauss divergence theorem:

$$F_{12} = \int_{A_{xy}} [P(x,y;z_1) - P(x,y;z_2)] \, dx dy. \tag{38}$$

A_{xy} is the cross-sectional area of the pore and F_{12} is the *total* frictional force in the z direction exerted on the pore wall from $z_1 \rightarrow z_2$ by the fluid as it moves through the pore. Combining Eqs. 36 and 38 gives

$$F_{12}/A_{xy} = P_0(z_1) - P_0(z_2) - [\Pi_0(z_1) - \Pi_0(z_2)][1 - \Phi e^{V_0}], \tag{39}$$

where the solute distribution coefficient Φ is identically equal to $(1/A_{xy}) \int_{A_{xy}} e^{-V} \, dx \, dy$. If we take z_1 and z_2 to be the pore ends (bulk solution – membrane interfaces), then Eqs. 16 *A–D* may be used to substitute bulk quantities and Eq. 39 becomes

$$F_{0l}/A_{xy} = \Delta P_\infty - (1 - \Phi)\Delta\Pi_\infty. \tag{40}$$

Thus, for a cylindrical pore of arbitrary cross section the fluid-membrane friction resulting from osmotic flow depends only on the first power of the solute exclusion, $(1 - \Phi)$.

The above result could be quite misleading. Suppose it is proposed that the flow rate is directly proportional to the friction between fluid and interior membrane surface. Eq. 40 then *seems* to imply

$$J_v = k(F_{0l}/A_{xy}) = k[\Delta P_\infty - (1 - \Phi)\Delta\Pi_\infty] \tag{41}$$

and hence $\sigma_0 = 1 - \Phi$. This argument must be fallacious since we know that $\sigma_0 = (1 - \Phi)^2$ for a circular cross section with only steric solute-wall interactions. An explanation of this apparent paradox is readily found by comparing the velocity profiles for pressure-driven and osmotic-driven flow. With pressure-driven flow the axial pressure gradient is uniform in any cross section (36) and it can be shown that such a condition leads to the most "efficient" flow field (parabolic), that is, $\bar{U}$ (or J_v) is a maximum for a given total driving force ΔP_∞. In the case of osmotic flow, however, the driving force $(1 - \Phi)\,\Delta\Pi_\infty$ is confined to an annular region adjacent to the pore wall and results in a less efficient flow profile. That is to say, the ratio of average velocity to total viscous friction at the pore wall is greater for pressure-driven flow than for osmotic-driven flow due to the steeper velocity gradient at the wall for the latter. It should be obvious from this discussion that fluid-membrane friction and

volumetric flow rate are not uniquely related independent of pore structure. Furthermore, Eqs. 20 and 40 show that at zero volume flow a net force must be impressed on a membrane consisting of circular cylindrical pores:

$$J_v = 0 \Rightarrow \Delta P_\infty = (1 - \Phi)^2 \Delta \Pi_\infty, \tag{42A}$$

$$F_{0l}/\pi r_w^2 = -\Phi(1 - \Phi)\Delta \Pi_\infty. \tag{42B}$$

Only for a semipermeable membrane ($\Phi = 0$) is a true mechanical equilibrium established axially at $J_v = 0$. In summary, the failure of Eq. 40 to yield a reflection coefficient can be attributed to the fundamental hydrodynamic differences between pressure-driven and osmotic-driven flows, i.e. the two driving forces are *not* mechanistically equivalent for membranes with cylindrical pores and probably not for heterogeneous membranes in general. This result seriously challenges the validity of one-dimensional analyses of osmotic transport as formulated heretofore.

Often a porous membrane is described by a matrix of interconnected fibers which form the continuous solid phase. Although such a model is much less amenable to analysis than a pore of constant cross section, the concept that osmotic flow results from a coupling between concentration and pressure due to thermodynamic interaction between solute and fiber surface at least provides the proper phenomenological insight from which to proceed toward deriving expressions relating σ_0 to solute and membrane physical characteristics. It is in fact this insight which is lost in any lumped parameter, one-dimensional model. Manning (11) proceeds from the *assumption* that one can *define* a solute potential $V_a(z)$, which has been somehow averaged over the plane normal to the transport direction (z), a potential which simultaneously satisfies the kinetic and mechanical equilibrium requirements of Eq. 3 as well as describes solute distribution between membrane and bulk solutions. However, he makes no attempt to explain how the potential is related to membrane and solute parameters, nor how the averaging of potential should be performed. While we do not challenge his analysis *given* this assumption, we do question the validity of such an assumption for rigid, porous membranes. Specifically, his general model should be capable of correctly relating σ_0 and Φ for a membrane composed of circular capillaries. That this is not the case is demonstrated by Eq. 54[3] in his paper (11) which is derived for a potential V_a which is independent of z:

$$\sigma_0 = 1 - \Phi.$$

This expression disagrees with Eq. 20, the latter obtained from direct solution of the Navier-Stokes equation. Furthermore, his analysis predicts mechanical equilibrium along the transport direction at $J_v = 0$ (implying zero viscous energy dissipation), a

[3]Eq. 54 in Manning's paper (11) is proposed for a locally homogeneous membrane, but the analysis leading to it is applicable to a heterogeneous membrane as long as $V_a \neq V_a(z)$, e.g., a capillary pore membrane. For a general, heterogeneous membrane his equation 7*b* is obtained: $\sigma_0 = 1 - \kappa\Phi$ where κ is an averaged periodic partition function which equals unity for a uniformly constant potential.

misconceived notion discussed earlier in this paper. Thus, there is no reason a priori to expect that the one-dimensional approach can accurately relate reflection coefficient and distribution coefficient for a membrane of arbitrary pore structure. A similar conclusion is reached by Anderson and Quinn (15) regarding the adequacy of one-dimensional models for describing hindered diffusion and filtration in microporous systems. Manning states that his general model can be extended by using a three-dimensional potential function without difficulty but would lead to no significantly different conclusions. The results of such an extension, as reported here, show that in fact the extra dimensionality leads to quite different conclusions. Furthermore, three-dimensional considerations require simultaneous solution of the Navier-Stokes equation, far from a simple matter except for the simplest of geometries.

SUMMARY

The basic principle behind osmotic flow is that impermeable surfaces within a porous membrane create gradients in solution properties normal to these surfaces which are necessary to maintain thermodynamic equilibrium. If the boundary interacts differently with the solute than with the solvent and such an interaction can be described by a potential energy, then pressure and concentration are related by the Gibbs-Duhem equation. It is this rather important fundamental appreciation of the vectorial nature of both thermodynamic equilibrium and transport processes which is sacrificed in a one-dimensional analysis. As a consequence, pore geometry cannot be neglected when interpreting the physical significance of a measured reflection coefficient. The results presented here are specific for cylindrical pores of circular cross section, and applicability to other geometries is uncertain at the present time. A more fundamental shortcoming, however, is the assumption of continuum properties for the solvent since limitations are then placed on the smallest pore size to which the equations can be applied with confidence. For pores not much larger than the solvent molecule a single potential function is probably insufficient to describe the wall effect because solute-solvent interactions may be different from those in the bulk solution (see Manning [11]), contrary to the assumptions made here. A further difficulty with such small pores is that a molecular theory of viscous transport may be required to relate fluid flow to pressure gradient (23, 24).

Despite the restrictions of pore size and geometry which limit the quantitative usefulness of Eqs. 17 *B*, 19, and 20, the basic mechanism proposed here for osmotic flow is generally valid for all rigid, heterogeneous membranes. Steric factors prevent the larger solute molecule from approaching the interior membrane solid surfaces as close as the solvent, thereby creating a solvent-rich region near the wall. Thermodynamic equilibrium requires the pressure to be lower in this region than in the adjacent solution; thus, a solute concentration gradient tangent to the surface establishes a pressure gradient in the opposite direction. For a cylindrical pore of circular cross section the resulting bulk flow has a rather flat velocity profile in the region accessible to the solute, differing significantly in shape from the classical pressure-driven velocity pro-

file. For neutral spherical solutes in such pores σ_0 is given by Eqs. 19 and 20; the effect of a nonspherical shape is to increase σ_0 toward unity, as illustrated in Fig. 4. The existence of attractive forces between solute and pore wall (weak adsorption), as long as the solute retains mobility, reduces the reflection coefficient and may even result in a negative value as seen in Figs. 5 and 6. Values of σ_0 closer to unity than expected from steric factors alone should be observed if the solute-wall interaction is repulsive. If the nonsteric potential (V^*) is concentration as well as position dependent, as for the case of electrolytes in charged pores, then the analysis is considerably more difficult since simultaneous solution of the momentum and solute transport equations is required.

LIST OF SYMBOLS

a	Mean solute radius (see Giddings et al. [10]) (cm).
a_1	One-half length of capsule-shaped solute (cm).
a_2	Radius of body and cap of capsule-shaped solute (cm).
A	Adsorption potential constant (Eq. 33) (cm^n).
A_{xy}	Cross-sectional area of a cylindrical pore (cm^2).
B	Integral defined by Eq. 14 B (cm^4).
C	Solute concentration (mol/cm^3).
f_{ij}	Friction coefficient between components i and j (g/s per mol i).
F_{0l}	Total viscous frictional force exerted by a fluid on the pore wall under simultaneous pressure and osmotic driving forces (Eq. 40) (dyn).
$G(r)$	Lag coefficient for a particle situated at position r in a laminar flow field within a capillary.
$\bar{G}$	An averaged value of $G(r)$ over the pore cross section (see Anderson and Quinn [14]).
G_0	$G(0)$.
J_s	Solute flux through the membrane (mol/cm^2 per s).
J_v	Total volume flux through the membrane (cm/s).
l	Pore length (cm).
L_p	The hydraulic coefficient, $\alpha r_0^2/8\eta l$ for a cylindrical pore geometry ($cm^2 \times s/g$).
n	Exponent for dispersion energy (Eq. 33).
P	Pressure (dyn/cm^2).
r	Radial position within the pore (cm).
r_w	Pore radius (cm).
$S(x)$	Step function: equals zero if $x < 0$, equals one if $x \geq 0$.
$U(r,z)$	Fluid velocity (z direction) in the pore (cm/s).
$\bar{U}$	Average value of U over the pore area (cm/s).
$\vec{U}$	Three-dimensional fluid velocity vector in the pore, (cm/s).
$V(r)$	$\phi(r)/RT$.
$V^*(r)$	The nonsteric (adsorption) contribution to $V(r)$.
$V_a(z)$	Membrane area-averaged dimensionless solute potential which may vary along the transport direction (Manning [11]).
W	Fluid velocity in the radial direction in the pore (cm/s).
x,y	Dummy variables of integration (Eq. 13), or rectilinear coordinates in the cross section of a pore of arbitrary boundary (Eq. 36) (cm).
z	Axial position along the pore (cm).
α	Pore volume fraction of the membrane.

$\beta(a,\Psi)$ Closest approach of the solute center of mass to the pore wall when oriented at angles Ψ (cm).

$\delta(a,\Psi)$ Deviation defined in Eq. 27.

ϵ Solute eccentricity, a_2/a_1.

η Fluid viscosity (g/cm per s).

λ a/r_0.

Π Osmotic pressure = RTC (dyn/cm^2).

σ_0 Osmotic reflection coefficient (Eq. 3)

σ_f Filtration reflection coefficient (Eq. 4).

$\phi(r)$ Solute potential energy within the pore (ergs/mol solute).

Φ Solute distribution coefficient between pore and bulk solutions, based on total pore volume.

Ψ Normalized representation of angular orientation of a solute molecule with respect to the z and r axes.

Subscripts

∞ Bulk solution.

0 Evaluation on pore center line $r = 0$ or in the bulk solution at $z = 0$.

l In the bulk solution at $z = l$.

c Core region accessible to solute (see Fig. 2).

e Excluded region inaccessible to solute.

Operators

$\vec{\nabla}$ Vector gradient (cm^{-1}).

∇^2 LaPlacian = $\vec{\nabla}\cdot\vec{\nabla}$ (cm^{-2}).

This work was supported in part by the National Science Foundation.

Received for publication 8 April 1974 and in revised form 22 August 1974.

REFERENCES

1. DENBIGH, K. 1966. The Principles of Chemical Equilibrium. Cambridge University Press, New York.
2. STAVERMAN, A. J. 1951. *Rec. Trav. Chim.* **70**:344.
3. KATCHALSKY, A., and P. F. CURRAN. 1965. Non-Equilibrium Thermodynamics in Biophysics. Harvard University Press, Cambridge, Mass.
4. SPIEGLER, K. S., and O. KEDEM. 1966. *Desalination.* **1**:311.
5. DE GROOT, S. R., and P. MAZUR. 1962. *Non-Equilibrium Thermodynamics.* North-Holland Publishing Co., Amsterdam.
6. MAURO, A. 1957. *Science (Wash. D.C.).* **126**:252.
7. ROBBINS, E., and A. MAURO. 1960. *J. Gen. Physiol.* **43**:523.
8. MAURO, A. 1960. *Circulation.* **21**:845.
9. RAY, P. M. 1960. *Plant Physiol.* **35**:783.
10. GIDDINGS, J. C., E. KUCERA, C. P. RUSSELL, and M. N. MYERS. 1968. *J. Phys. Chem.* **72**:4397.
11. MANNING, G. S. 1968. *J. Chem. Phys.* **49**:2668.
12. FERRY, J. D. 1936. *Chem. Rev.* **18**:373.
13. RENKIN, E. M. 1954. *J. Gen. Physiol.* **38**:225.
14. BEAN, C. P. 1972. Physics of porous membranes. *In* Membranes: A Series of Advances. Vol. 1. G. Eisenman, editor. Marcel Dekker, New York.
15. ANDERSON, J. L., and J. A. QUINN. 1974. *Biophys. J.* **14**:130.
16. BEARMAN, R. J., and J. G. KIRKWOOD. 1958. *J. Chem. Phys.* **28**:136.
17. SPIEGLER, K. S. 1958. *Trans. Faraday Soc.* **54**:1408.

18. KEDEM, O., and A. KATCHALSKY. 1958. *Biochim. Biophys. Acta.* **27**:229.
19. DAINTY, J., and B. Z. GINZBURG. 1963. *J. Theor. Biol.* **5**:256.
20. PERL, W. 1973. *Microvasc. Res.* **6**:169.
21. MIKULECKY, D. C. 1972. *Biophysical J.* **12**:1642.
22. HILL, A. E. 1972. *J. Theor. Biol.* **36**:255.
23. LONGUET-HIGGINS, H. C., and G. AUSTIN. 1966. *Biophys. J.* **6**:217.
24. LEVITT, D. G. 1973. *Biophys. J.* **13**:186.
25. DERJAGUIN, B. V., S. S. DUKHIN, and M. M. KOPTELOVA. 1972. *J. Colloid Interface Sci.* **38**:584.
26. WANG, H., and R. SKALAK. 1969. *J. Fluid Mech.* **38**:75.
27. BEARMAN, R. J. 1960. *J. Chem. Phys.* **32**:1308.
28. WYMAN, C. E., and M. O. KOSTIN. 1973. *J. Chem. Phys.* **59**:3411.
29. APFEL, R. E. 1972. *Sci. Am.* **227(6)**:58.
30. SCHOLANDER, P. F. 1972. *Am. Sci.* **60**:584.
31. MAURO, A. 1965. *Science (Wash. D.C.).* **149**:867.
32. ONSAGER, L. 1931. *Phys. Rev.* **37**:405.
33. FITTS, D. D. 1962. Nonequilibrium Thermodynamics. McGraw-Hill, New York. 39–40.
34. GYARMATI, I. 1970. Non-Equilibrium Thermodynamics. Springer-Verlag, New York. 85.
35. TRUESDELL, C. A. 1969. Rational Thermodynamics–A Course of Lectures on Selected Topics. McGraw-Hill, New York.
36. HAPPEL, J., and H. BRENNER. 1965. Low Reynolds Number Hydrodynamics, Prentice-Hall, Englewood Cliffs, N.J.
37. VERWEY, E. J., and J. T. G. OVERBEEK. 1948. Theory of the Stability of Lyophobic Colloids. Elsevier, New York.
38. TALEN, J. L., and A. J. STAVERMAN. 1965. *Trans. Faraday Soc.* **61**:2800.
39. SOLOMON, A. K. 1968. *J. Gen. Physiol.* **51**:335*s*.
40. BIRD, R. B. 1957. *Chem. Eng. Sci.* **6**:123.

APPENDIX

Equation of Motion

Assuming angular uniformity and slow viscous flow, the Navier-Stokes equations for the axial (U) and radial (W) velocities are:

$$-\frac{\partial P}{\partial z}+\frac{\eta}{r}\frac{\partial}{\partial r}\left(r\frac{\partial U}{\partial r}\right)+\eta\frac{\partial^2 U}{\partial z^2}=0, \tag{43}$$

$$-\frac{\partial P}{\partial r}-\frac{C\,\mathrm{d}\phi}{\mathrm{d}r}+\eta\frac{\partial}{\partial r}\left[\frac{1}{r}\frac{\partial}{\partial r}(rW)\right]+\eta\frac{\partial^2 W}{\partial z^2}=0. \tag{44}$$

The equation of mass continuity for an incompressible fluid is

$$(1/r)(\partial/\partial r)(rW)+(\partial U/\partial z)=0. \tag{45}$$

By nondimensionalizing the coordinates in defining $\zeta \equiv r/r_0$ and $\xi \equiv z/l$, Eqs. 43 and 44 become

$$-\frac{\partial P}{l\partial\xi}+\frac{\eta}{r_w^2}\left[\frac{1}{\zeta}\frac{\partial}{\partial\zeta}\left(\zeta\frac{\partial U}{\partial\zeta}\right)+\left(\frac{r_w}{l}\right)^2\frac{\partial^2 U}{\partial\xi^2}\right]=0, \tag{46}$$

$$-\frac{\partial P}{r_w\partial\zeta}-\frac{C\,\mathrm{d}\phi}{r_w\,\mathrm{d}\zeta}+\frac{\eta}{r_w^2}\left[\frac{\partial}{\partial\zeta}\left(\frac{1}{\zeta}\frac{\partial}{\partial\zeta}(\zeta W)\right)+\left(\frac{r_w}{l}\right)^2\frac{\partial^2 W}{\partial\xi^2}\right]=0. \tag{47}$$

If $(r_w/l)^2 \ll 1$, the gradients along the axial direction become unimportant compared to radial gradients. Thus, Eq. 46 is approximated by Eq. 11 with negligible error. Neglecting the axial derivative in Eq. 47 and using the continuity relation, Eq. 45, the radial component is simplified to

$$\left[\frac{\partial P}{\partial \zeta} + C\frac{d\phi}{d\zeta}\right] + \frac{\eta}{l}\frac{\partial^2 U}{\partial \zeta \partial \xi} = 0. \tag{48}$$

By dimensional arguments the ratio of the kinetic term to one of the terms in brackets above is given by

$$\left(\frac{\eta}{l}\frac{\partial^2 U}{\partial \zeta \partial \xi}\right)\Big/\frac{\partial P}{\partial \zeta} \sim \frac{\eta \bar{U}/l}{\Delta P} \sim \frac{(\eta/l)(r_w^2 \Delta P/8\eta l)}{\Delta P} = \frac{1}{8}\left(\frac{r_w}{l}\right)^2.$$

Thus, as $(r_w/l)^2 \to 0$ the kinetic term becomes insignificant and the assumption of radial mechanical equilibrium (Eq. 8) is valid.

Assumption of Radial Thermodynamic Equilibrium

The approach to thermodynamic equilibrium is governed by the rate of mass transfer. For equilibrium to be established the radial diffusive velocity of solute must be larger than the flow velocity which tends to disrupt equilibrium:

$$D/r_w \gg W, \tag{49}$$

where D is the effective solute diffusion coefficient. Through continuity the average radial velocity ($\bar{W}$) is related to the average axial velocity by

$$\bar{W} \sim (r_w/l)\bar{U}, \tag{50}$$

and so

$$r_w^2 \ll Dl/\bar{U}. \tag{51}$$

If the Peclet number (Pe) is defined as $\bar{U}l/D$, then

$$(r_w/l)^2 \ll 1/Pe. \tag{52}$$

The above represents the sufficient criterion for assuming radial thermodynamic equilibrium. What it says is simply the following: the pore must be narrow enough to allow the solute to distribute itself (by diffusion) rapidly enough in the radial direction to overcome the small radial velocity which tends to disturb the concentration profile away from the Boltzmann distribution.